Polyelectrolyte-Multilayer-Supported Au@Ag Core-Shell Nanoparticles with High Catalytic Activity

*Xin Zhang and Zhaohui Su**

Bimetallic nanoparticles (NPs) composed of noble metals including Au, Ag, Pt, and Pd have attracted extensive research interest in recent years due to their composition-dependent optical, electronic, and catalytic properties, which lead to a wide range of applications such as surface-enhanced Raman scattering, sensors, and catalysis.[1–3] In the field of catalysis in particular, bimetallic NPs are of great importance because they often show better catalytic performance than their corresponding monometallic counterparts and bulk materials.[4] However, in practical applications, without a suitable support, metallic NPs can easily aggregate, which results in substantial reduction in catalytic activity. An effective strategy to prevent aggregation is to immobilize metallic NPs on supports such as carbon materials and metal-organic frameworks,[5,6] or in various polymer matrices,[7–21] including polyelectrolyte multilayers (PEMs). PEMs can be fabricated on a variety of substrates of different sizes and shapes facilely via the layer-by-layer assembly technique, and the film composition and thickness can be manipulated conveniently by controlling the assembly conditions.[22] Various monometallic NPs such as Au, Ag, Pt and Pd have been incorporated into PEMs, and the composite films have found applications in antimicrobial coatings, catalysis and electrocatalysis.[11–21] Recently, fabrication of Au-Ag alloy NPs in PEMs composed of weak polyelectrolytes was reported by several groups, with $AuCl_4^-$ and Ag^+ ions both introduced into the PEM and then reduced simultaneously.[23,24] In this communication, we report for the first time the in situ synthesis of Au@Ag core-shell NPs in PEMs and show that they exhibit superior catalytic activity for the reduction of 4-nitrophenol than monometallic Au or Ag NPs. This example demonstrates a general strategy for sequential introduction of oppositely charged species into a PEM by altering the capping layer.

Two typical polyelectrolytes, poly(styrene sulfonate) (PSS) and poly(diallyldimethylammonium chloride) (PDDA), were used for PEM construction. It is well known that when the PEM is capped with PDDA, the major salt ion present in the film is the counter anion, Cl^- in this case, which can then be exchanged by $AuCl_4^-$, a precursor for Au NPs; whereas for the PEMs capped with PSS, most of the small ions present in the PEMs are cations (Na^+), which can be exchanged by Ag^+ to synthesize Ag NPs.[15,25] In either case, the Na^+ or Cl^- counter ions are re-generated in the reduction step, therefore the ion-exchange/reduction cycle can be repeated multiple times to improve the loading and/or size of the metal NPs in the PEM,[14,15] with the loading proportional to the number of exchange/reduction cycles.[15] First, following a reported procedure a $(PDDA/PSS)_4PDDA$ film was assembled on a cleaned glass or quartz substrate, and Au NPs were introduced into the film via an anion exchange/reduction process.[15] A strong reducing agent, $NaBH_4$, was used in the first reduction cycle to generate Au NPs as seeds, and in all subsequent reductions (including that for Ag) ascorbic acid, a weak reducing agent, was used so that the reduction only occurred on the existing metal NPs, resulting in more uniform and sequential NP growth. Onto the PEM that had undergone two exchange/reduction cycles, denoted $(PDDA/PSS)_4PDDA/2Au$, was deposited a PSS layer and the PEM became $(PDDA/PSS)_5/2Au$. The Au-loaded PEM with a PSS capping layer was then subjected to counter cation exchange/reduction cycles to load Ag into the film.[25] The process was monitored by X-ray photoelectron spectroscopy (XPS). As seen in **Figure 1**a, the Na 1s peak, absent in the spectrum of $(PDDA/PSS)_4PDDA$, emerges at 1072 eV for the $(PDDA/PSS)_5/2Au$ film, which is a good indication that the PEM is now terminated with a PSS layer and that the dominant counter ion has been switched from an anion to a cation. After incorporation of Ag in two cation-exchange/reduction cycles, which yields $(PDDA/PSS)_5/2Au@2Ag$, the Ag 3d doublet is clearly identified at 368.4 and 374.4 eV (Supporting Information), indicative of presence of metallic Ag. Meanwhile the intensity of the Au 4f doublet, located at 84.1 and 87.9 eV (Supporting Information, Figure S1) corresponding to Au in its zero-valent state, is significantly reduced. These results suggest that both Au and Ag are present in the PEM, with Au NPs coated with Ag, forming core-shell structures, and the photoelectrons generated by the Au cores are partially screened by the Ag shells.

Figure 1b shows the UV–vis spectra of Au, Ag and Au-Ag NPs embedded in the PEMs. For $(PDDA/PSS)_5$ films loaded with Au and Ag NPs, the surface plasmon resonance (SPR) peak emerges at 535 nm and 429 nm, respectively, confirming the formation of Au and Ag NPs in the PEM matrices. For the PEM containing both Au and Ag, however, a broad band with two components at around 500 and 400 nm is observed, which is similar to that reported for Au@Ag core-shell NPs.[26] This behavior is distinct from that of Au-Ag alloy NPs, which exhibits a single peak the position of which is dependent on the alloy composition.[27] On the other hand, a mixture of Au and Ag NPs would produce two SPR peaks in the positions corresponding to monometallic Au and Ag NPs,[27,28] which is

X. Zhang, Prof. Z. Su
State Key Laboratory of Polymer Physics and Chemistry
Changchun Institute of Applied Chemistry
Chinese Academy of Sciences
Changchun 130022, PR China
E-mail: zhsu@ciac.jl.cn
X. Zhang
Graduate School of the Chinese Academy of Sciences
Chinese Academy of Sciences
Changchun 130022, PR China

DOI: 10.1002/adma.201201712

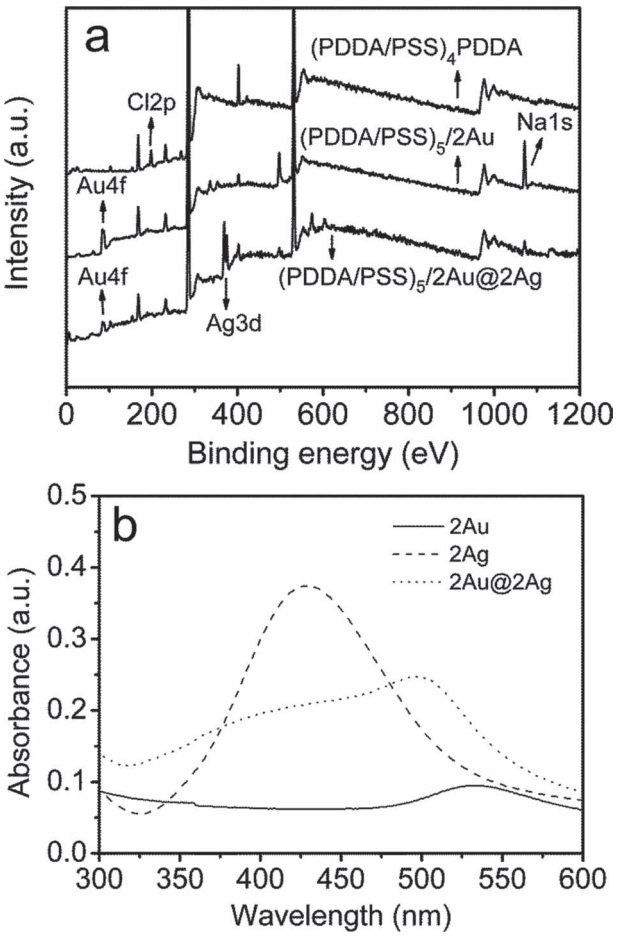

Figure 1. a) XPS spectra of $(PDDA/PSS)_4PDDA$, $(PDDA/PSS)_5/2Au$, and $(PDDA/PSS)_5/2Au@2Ag$, and b) UV–vis spectra of $(PDDA/PSS)_5/2Au$, $(PDDA/PSS)_5/2Ag$, and $(PDDA/PSS)_5/2Au@2Ag$ composites.

not the case here either. Thus, the UV–vis data confirm that Au@Ag bimetallic core-shell NPs have been synthesized in the PEM. **Figure 2** shows a transmission electron micrograph (TEM) of the Au-Ag bimetallic NPs formed in the PEM. It can be seen that the NPs are largely spherical, and most exhibit inhomogeneous electron density with a dark core coated by a light shell, which further verifies the core-shell structure of the Au-Ag bimetallic NPs.

Next, we examine the catalytic activity of the PEM-supported Au, Ag and Au@Ag core-shell NPs for the reduction of 4-nitrophenol into 4-aminophenol by $NaBH_4$. This reaction can be easily monitored by UV–vis absorption spectroscopy, and therefore is often chosen as a model reaction to evaluate the catalytic activities of various metallic NPs including Cu,[29] Ni,[30] Au,[9] Ag,[8] Pt,[31] and Pd.[32] After addition of $NaBH_4$ into 4-nitrophenol aqueous solution in the absence of a catalyst, the color of the solution quickly changed from light yellow to yellow green, and in the UV–vis spectrum a strong absorption peak shifted from 318 nm to 400 nm (Figure S2) due to the formation of 4-nitrophenolate anions under alkaline conditions.[33] The intensity of this peak remained unchanged with time because the reduction reaction cannot proceed without

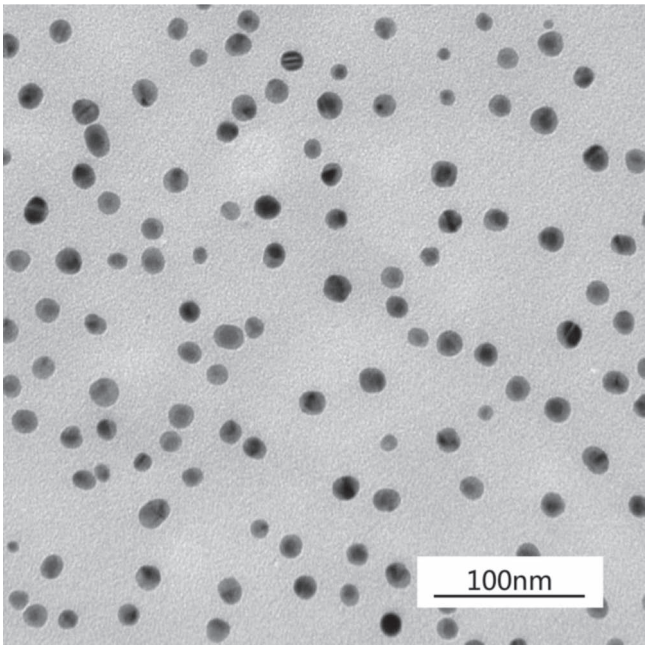

Figure 2. TEM image of 2Au@4Ag NPs dispersed in a $(PDDA/PSS)_3$ film.

a catalyst.[5] Then a PEM deposited on a quartz substrate and loaded with metal NPs was introduced to catalyze the reduction, and the reaction kinetics was followed by monitoring the reaction solution by UV–vis absorption spectroscopy. **Figure 3**a displays the time-dependent UV–vis absorption spectra, which show that the absorption peak of 4-nitrophenol at 400 nm decreases with time and a new peak at 300 nm concomitantly appears after addition of PEM-supported metallic NPs catalyst, which indicates the conversion of 4-nitrophenol into 4-aminophenol. In this catalytic reaction, because $NaBH_4$ was in large excess compared to 4-nitrophenol, the reaction rate was roughly independent of the $NaBH_4$ concentration, and the kinetics can be considered pseudo-first-order with respect to 4-nitrophenol. The experiments were carried out under identical conditions for three different kinds of NPs, 2Au, 2Ag, and 2Au@2Ag. The mass of Au and Ag in $(PDDA/PSS)_5/2Au@2Ag$ should be the same as that in $(PDDA/PSS)_5/2Au$ and $(PDDA/PSS)_5/2Ag$, respectively.[15] Figure 3b plots $\ln(A_t/A_0)$ as a function of reaction time for three different NP catalysts, where A_t and A_0 is the peak intensity at time t and 0, respectively. The linear relationship confirms the pseudo-first-order kinetics, and the kinetic rate constant is estimated from the slope to be 0.019, 0.069, and 0.18 min^{-1} for 2Au, 2Ag, and 2Au@2Ag respectively. These results indicate that Au-Ag bimetallic NPs have higher catalytic activity than the corresponding monometallic NPs and the sum of the two, probably due to synergistic effects between Au and Ag, consistent with the conclusion of a recent study on Au@Ag core-shell NPs stabilized on metal-organic framework.[6]

In summary, we have developed a facile route for the in situ synthesis of Au-Ag core-shell NPs in multilayer thin films through a successive ion-exchange/reduction process. These bimetallic core-shell NPs in the composite thin films exhibit better catalytic performance than the corresponding monometallic ones. In the synthesis process, addition of a

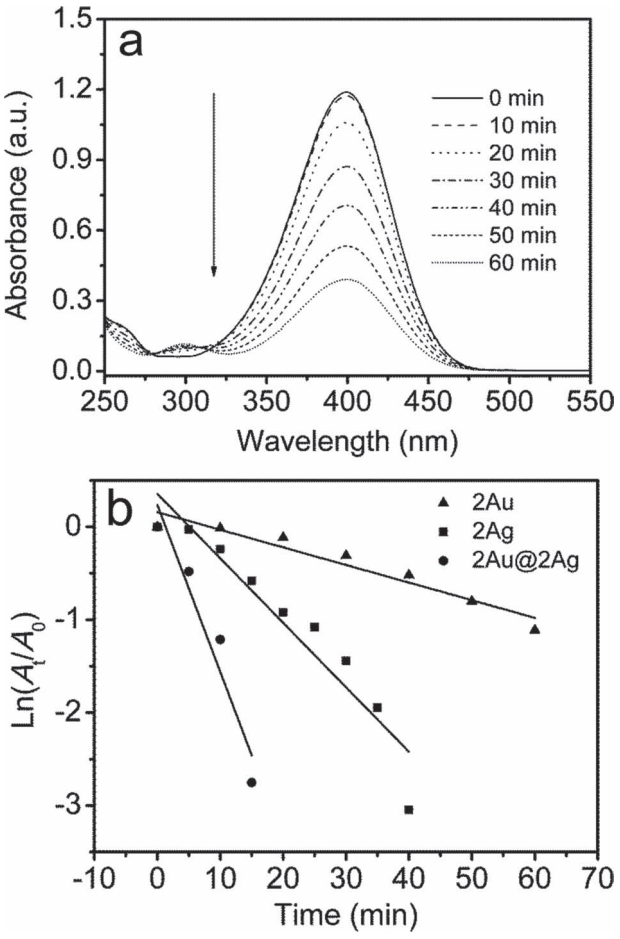

Figure 3. a) Time-dependent UV–vis absorption spectra of the reduction of 4-nitrophenol by $NaBH_4$ in the presence of $(PDDA/PSS)_5$/2Au. b) Plot of $\ln(A_t/A_0)$ as a function of time for the reaction catalyzed by $(PDDA/PSS)_5$/2Au, $(PDDA/PSS)_5$/2Ag, and $(PDDA/PSS)_5$/2Au@2Ag.

polyelectrolyte layer can switch the dominant type of counter ion so that metal precursor ions of different charge types can be introduced sequentially. This feature makes PEMs extremely versatile for in situ synthesis of metal NPs of different sizes, compositions and structures for optimum performance in catalysis and other applications.

Experimental Section

Materials: Chloroauric acid tetrahydrate ($HAuCl_4{\cdot}4H_2O$) and silver nitrate ($AgNO_3$) were purchased from Sinopharm Chemical Reagent Co., Ltd. Sodium chloride (NaCl) and 4-nitrophenol were purchased from Beijing Chemical Reagents Company. Ascorbic acid was purchased from Huishi Biochemical Co., Ltd. (Shanghai, China). PDDA (20 wt% in water, MW ≈ 200 000–350 000 g mol^{-1}), PSS (MW ≈ 70 000 g mol^{-1}) and sodium boronhydride ($NaBH_4$) were purchased from Aldrich. All of the chemicals were used as received without further purification. Ultrapure water (18.2 MΩ cm) was purified using a Millipore Simplicity system and used in all of the experiments.

Preparation of $(PDDA/PSS)_n$ Film: Quartz and glass slides were cleaned in a boiling piranha solution (H_2SO_4/H_2O_2 = 70:30 v/v) and subsequently rinsed with copious amounts of ultrapure water. A $(PDDA/PSS)_n$ film was assembled by sequential dipping of the substrate into PDDA (1.0 mg/mL) and PSS (1.0 mg/mL) aqueous solutions for 30 min each until the desired number of bilayers was obtained. Every dipping was followed by sufficient water rinsing. NaCl of 1.5 M concentration was maintained in all polyelectrolyte solutions.

Synthesis of aAu@bAg: A $(PDDA/PSS)_n$PDDA film was dipped into a $HAuCl_4$ solution (1 mM) for 5 min, removed and rinsed with water, and then treated with a freshly prepared aqueous solution of $NaBH_4$ (0.1 M, for the first reduction only) or ascorbic acid (0.1 M, for all subsequent reductions) for 5 min. This exchange/reduction reaction cycle was repeated for certain times to produce a PEM loaded with Au NPs. PEMs loaded with Ag NPs were synthesized from $(PDDA/PSS)_n$ films and $AgNO_3$ solution (10 mM) using the same protocol. Then a layer of PSS was deposited following the assembly procedure described above onto the $(PDDA/PSS)_n$PDDA film loaded with Au NPs. Next the $(PDDA/PSS)_{n+1}$ film was dipped into an $AgNO_3$ solution (10 mM) for 5 min, removed and rinsed with water, and then treated with a freshly prepared aqueous solution of ascorbic acid (0.1 M) for 5 min. This exchange/reduction reaction cycle was repeated for certain times. The bimetallic NPs are denoted *a*Au@*b*Ag for short, where *a*, and *b* are the numbers of exchange/reduction reaction cycles for Au and Ag, respectively.

Characterization: UV–vis spectra of the PEMs containing metallic NPs deposited on quartz slides were acquired on a TU-1901 spectrometer (Beijing Purkinje General Instrument Co., Ltd.). Transmission electron microscopy (TEM) measurements were carried out on a JEOL JEM-1011 microscope operating at an accelerating voltage of 100 kV. A small piece of PEM film containing metallic NPs was peeled from the substrate in hydrofluoric acid, floated in ultrapure water, and transferred to carbon-coated copper grids for TEM characterization. X-ray photoelectron spectroscopy (XPS) was performed on a Thermo-Electron ESCALAB 250 spectrometer, using monochromatic Al Kα radiation as the X-ray source for excitation. The spectra were recorded at a 90° takeoff angle and 20 eV pass energy. The binding energies of all of the peaks were referenced to a C1s value of 284.6 eV.

Catalytic Reactions with PEM-Supported Metallic NPs: The rate of 4-nitrophenol reduction was evaluated using UV–vis spectroscopy. For this purpose, one side of the quartz slide was covered with PEM-supported metallic nanoparticles and the slide was placed in a quartz cuvette filled with a mixed solution of 2 mL $NaBH_4$ (10 mM) and 1 mL 4-nitrophenol (0.2 mM). The slide was positioned such that it did not block the beam path. Ultrapure water was used as the reference. The absorbance of the solution was recorded in a scanning range of 250–550 nm with several min intervals. All of the experiments were carried out at room temperature without stirring.

Supporting Information

Supporting Information is available from the Wiley Online Library or from the author.

Acknowledgements

This work was supported by the National Natural Science Foundation of China (21174145). Z.S. thanks the NSFC Fund for Creative Research Groups (50921062) for support.

Received: April 28, 2012
Revised: June 22, 2012
Published online: July 16, 2012

[1] N. Toshima, T. Yonezawa, *New J. Chem.* **1998**, *22*, 1179.
[2] D. S. Wang, Y. D. Li, *Adv. Mater.* **2011**, *23*, 1044.
[3] R. G. Chaudhuri, S. Paria, *Chem. Rev.* **2012**, *112*, 2373.
[4] H. L. Jiang, Q. Xu, *J. Mater. Chem.* **2011**, *21*, 13705.
[5] S. C. Tang, S. Vongehr, X. K. Meng, *J. Mater. Chem.* **2010**, *20*, 5436.

[6] H. L. Jiang, T. Akita, T. Ishida, M. Haruta, Q. Xu, *J. Am. Chem. Soc.* **2011**, *133*, 1304.
[7] R. M. Crooks, M. Q. Zhao, L. Sun, V. Chechik, L. K. Yeung, *Acc. Chem. Res.* **2001**, *34*, 181.
[8] Y. Lu, Y. Mei, M. Drechsler, M. Ballauff, *Angew. Chem.* **2006**, *118*, 827; *Angew. Chem. Int. Ed.* **2006**, *45*, 813.
[9] J. Han, L. Y. Li, R. Guo, *Macromolecules* **2010**, *43*, 10636.
[10] C. Sivakumar, K. L. Phani, *Chem. Commun.* **2011**, *47*, 3535.
[11] T. C. Wang, M. F. Rubner, R. E. Cohen, *Langmuir* **2002**, *18*, 3370.
[12] K. K. Chia, R. E. Cohen, M. F. Rubner, *Chem. Mater.* **2008**, *20*, 6756.
[13] D. Lee, R. E. Cohen, M. F. Rubner, *Langmuir* **2005**, *21*, 9651.
[14] X. J. Zan, Z. H. Su, *Thin Solid Films* **2010**, *518*, 5478.
[15] X. Zhang, X. J. Zan, Z.H. Su, *J. Mater. Chem.* **2011**, *21*, 17783.
[16] J. H. Dai, M. L. Bruening, *Nano Lett.* **2002**, *2*, 497.
[17] S. Kidambi, J. Dai, J. Li, M. L. Bruening, *J. Am. Chem. Soc.* **2004**, *126*, 2658.
[18] D. M. Dotzauer, J. H. Dai, L. Sun, M. L. Bruening, *Nano Lett.* **2006**, *6*, 2268.
[19] D. M. Dotzauer, S. Bhattacharjee, Y. Wen, M. L. Bruening, *Langmuir* **2009**, *25*, 1865.
[20] L. Ouyang, D. M. Dotzauer, S. R. Hogg, J. Macanas, J. F. Lahitte, M. L. Bruening, *Catal. Today* **2010**, *156*, 100.
[21] H. F. Li, S. Y. Gao, Z. L. Zheng, R. Cao, *Catal. Sci. Technol.* **2011**, *1*, 1194.
[22] G. Decher, J. B. Schlenoff, in *Multilayer Thin Films: Sequential Assembly of Nanocomposite Materials*, Wiley-VCH, Weinheim, Germany **2003**.
[23] L. Shang, L. H. Jin, S. J. Guo, J. F. Zhai, S. J. Dong, *Langmuir* **2010**, *26*, 6713.
[24] M. A. Rahim, B. Nam, W. S. Choi, H. J. Lee, I. C. Jeon, *J. Mater. Chem.* **2011**, *21*, 11831.
[25] X. J. Zan, Z. H. Su, *Langmuir* **2009**, *25*, 12355.
[26] L. Chuntonov, M. Bar-Sadan, L. Houben, G. Haran, *Nano Lett.* **2012**, *12*, 145.
[27] M. P. Mallin, C. J. Murphy, *Nano Lett.* **2002**, *2*, 1235.
[28] C. M. Gonzalez, Y. Liu, J. C. Scaiano, *J. Phys. Chem. C* **2009**, *113*, 11861.
[29] Z. V. Feng, J. L. Lyon, J. S. Croley, R. M. Crooks, D. A. Vanden Bout, K. J. Stevenson, *J. Chem. Educ.* **2009**, *86*, 368.
[30] Z. M. Zhu, X. H. Guo, S. Wu, R. Zhang, J. Wang, L. Li, *Ind. Eng. Chem. Res.* **2011**, *50*, 13848.
[31] Y. Mei, G. Sharma, Y. Lu, M. Ballauff, M. Drechsler, T. Irrgang, R. Kempe, *Langmuir* **2005**, *21*, 12229.
[32] S. Harish, J. Mathiyarasu, K. L. N. Phani, V. Yegnaraman, *Catal. Lett.* **2009**, *128*, 197.
[33] Y. Shin, A. Dohnalkova, Y. H. Lin, *J. Phys. Chem. C* **2010**, *114*, 5985.